AMERICAN SOCIETY FOR MICROBIOLOGY | Applied and Environmental Microbiology®

ENVIRONMENTAL MICROBIOLOGY

Arcobacter peruensis sp. nov., a Chemolithoheterotroph Isolated from Sulfide- and Organic-Rich Coastal Waters off Peru

Cameron M. Callbeck,[a]* Chris Pelzer,[a,b] Gaute Lavik,[a] Timothy G. Ferdelman,[a] Jon S. Graf,[a] Bram Vekeman,[a] Harald Schunck,[c] Sten Littmann,[a] Bernhard M. Fuchs,[a] Philipp F. Hach,[a] Tim Kalvelage,[a] Ruth A. Schmitz,[c] Marcel M. M. Kuypers[a]

[a]Max Planck Institute for Marine Microbiology, Bremen, Germany
[b]Department of Microbiology, IWWR, Radboud University Nijmegen, Nijmegen, Netherlands
[c]Insitute for General Microbiology, University of Kiel, Kiel, Germany

ABSTRACT Members of the epsilonproteobacterial genus *Arcobacter* have been identified to be potentially important sulfide oxidizers in marine coastal, seep, and stratified basin environments. In the highly productive upwelling waters off the coast of Peru, *Arcobacter* cells comprised 3 to 25% of the total microbial community at a near-shore station where sulfide concentrations exceeded 20 μM in bottom waters. From the chemocline where the *Arcobacter* population exceeded 10^6 cells ml^{-1} and where high rates of denitrification (up to 6.5 ± 0.4 μM N day^{-1}) and dark carbon fixation (2.8 ± 0.2 μM C day^{-1}) were measured, we isolated a previously uncultivated *Arcobacter* species, *Arcobacter peruensis* sp. nov. (BCCM LMG-31510). Genomic analysis showed that *A. peruensis* possesses genes encoding sulfide oxidation and denitrification pathways but lacks the ability to fix CO_2 via autotrophic carbon fixation pathways. Genes encoding transporters for organic carbon compounds, however, were present in the *A. peruensis* genome. Physiological experiments demonstrated that *A. peruensis* grew best on a mix of sulfide, nitrate, and acetate. Isotope labeling experiments further verified that *A. peruensis* completely reduced nitrate to N_2 and assimilated acetate but did not fix CO_2, thus coupling heterotrophic growth to sulfide oxidation and denitrification. Single-cell nanoscale secondary ion mass spectrometry analysis of samples taken from shipboard isotope labeling experiments also confirmed that the *Arcobacter* population *in situ* did not substantially fix CO_2. The efficient growth yield associated with the chemolithoheterotrophic metabolism of *A. peruensis* may allow this *Arcobacter* species to rapidly bloom in eutrophic and sulfide-rich waters off the coast of Peru.

IMPORTANCE Our multidisciplinary approach provides new insights into the ecophysiology of a newly isolated environmental *Arcobacter* species, as well as the physiological flexibility within the *Arcobacter* genus and sulfide-oxidizing, denitrifying microbial communities within oceanic oxygen minimum zones (OMZs). The chemolithoheterotrophic species *Arcobacter peruensis* may play a substantial role in the diverse consortium of bacteria that is capable of coupling denitrification and fixed nitrogen loss to sulfide oxidation in eutrophic, sulfidic coastal waters. With increasing anthropogenic pressures on coastal regions, e.g., eutrophication and deoxygenation (D. Breitburg, L. A. Levin, A. Oschlies, M. Grégoire, et al., Science 359:eaam7240, 2018, https://doi.org/10.1126/science.aam7240), niches where sulfide-oxidizing, denitrifying heterotrophs such as *A. peruensis* thrive are likely to expand.

KEYWORDS chemolithoheterotrophy, denitrification, epsilonproteobacteria, nanoSIMS, sulfide oxidation, upwelling

Citation Callbeck CM, Pelzer C, Lavik G, Ferdelman TG, Graf JS, Vekeman B, Schunck H, Littmann S, Fuchs BM, Hach PF, Kalvelage T, Schmitz RA, Kuypers MMM. 2019. *Arcobacter peruensis* sp. nov., a chemolithoheterotroph isolated from sulfide- and organic-rich coastal waters off Peru. Appl Environ Microbiol 85:e01344-19. https://doi.org/10.1128/AEM.01344-19.

Editor Harold L. Drake, University of Bayreuth

Address correspondence to Timothy G. Ferdelman, tferdelm@mpi-bremen.de.

* Present address: Cameron M. Callbeck, Swiss Federal Institute of Aquatic Science and Technology (Eawag), Kastanienbaum, Switzerland.

Received 14 June 2019
Accepted 5 September 2019
Accepted manuscript posted online 4 October 2019
Published 27 November 2019

Communities of sulfide-oxidizing microorganisms in marine sulfide-rich environments, such as wood falls, seeps, and stratified water columns, often harbor large communities of the epsilonproteobacterial genus *Arcobacter* (1–8). The *Arcobacter* genus encompasses a diverse assemblage of species that include obligate and facultative chemolithoautotrophs as well as heterotrophs (see references 1, 9, and 10 and references therein). While much attention has focused on gut and food bearing pathogenic *Arcobacter* species, the *Arcobacter* genus also contains a wide variety of free-living, environmentally relevant species. For instance, the free-living species *Arcobacter butzleri*, which has been identified to be an enteropathogen, has also been isolated from aquatic environments (e.g., lakes) (11–14). *Arcobacter* spp. have been enriched in engineered systems containing high levels of sulfide and high levels of organic matter (9, 15–17), and *Arcobacter* spp. have been found in association with unicellular protists, where the *Arcobacter* spp. benefit from the transfer of labile organic matter and hydrogen (18). The metabolic capability to utilize reduced and intermediate-oxidation-state sulfur compounds for respiration as an electron donor (1, 11, 19) or even as an electron acceptor (10) appears to contribute to the ability of several *Arcobacter* spp. to thrive in marine, sulfur-rich (6, 20, 21) environments.

Sulfur-rich environments can be found in coastal upwelling systems, such as those off the coasts of Peru and Namibia, where large fluxes of organic carbon deposition drive enhanced rates of microbial sulfate reduction and sulfide production within the underlying sediments (22–25). During periods of sluggish water column circulation, dissolved hydrogen sulfide (H_2S and HS^-) diffuses out of the sediments and accumulates to concentrations often exceeding 20 μM in shelf bottom waters (6, 25–29). These sulfidic events represent extreme manifestations of coastal deoxygenation processes and contribute to the formation of anoxic dead zones (30–32). The occurrence of even low-micromolar concentrations of dissolved hydrogen sulfide restricts the availability of faunal habitat in hypoxic zones and eventually leads to a loss of faunal diversity and massive fish die-offs in otherwise productive, coastal upwelling systems (31–34). Counteracting the accumulation of hydrogen sulfide is the rapid oxidation of dissolved sulfide at redoxclines mediated by a variety of bacteria that use dissolved oxygen or nitrate as the terminal electron acceptor (6, 26, 27, 35, 36). The detection of abundant CO_2-fixing microbes in oxygen minimum zones (OMZs) and stratified basins, in concert with elevated rates of dark CO_2 fixation at sulfide-nitrate redoxclines, has led to the conclusion that chemolithoautotrophic bacteria are primarily responsible for the oxidation of sulfide (6, 26–29, 35, 37, 38). In addition to oxidizing sulfide to less toxic elemental sulfur or sulfate, many sulfide-oxidizing bacteria contribute to fixed nitrogen loss by coupling dissolved sulfide oxidation to denitrification (6, 26–28, 39, 40). *Arcobacter* has been identified to be a potentially important sulfide-oxidizing, denitrifying bacterium in the sulfide-rich waters off the coast of Namibia (6) and is hypothesized to serve a similar role in the sulfide-rich waters off the coast of Peru.

To further elucidate the role of *Arcobacter* associated with sulfidic events in marine ecosystems, we isolated a marine *Arcobacter* strain from a site in coastal, sulfidic Peruvian shelf waters, where *Arcobacter* spp. may comprise a substantial fraction of the bacterial community typically associated with sulfide oxidation. We analyzed the genome of the isolated *Arcobacter* and tested its physiology under conditions mimicking the Peru shelf environment from which it was isolated. In order to place the isolated *Arcobacter* in its environmental context, we examined the phylogenetic relationship of our isolated *Arcobacter* to the *in situ* populations of *Arcobacter* spp. and with respect to other sulfide-oxidizing chemolithotrophs. Lastly, we quantified the activity at the single-cell level of *in situ* populations of *Arcobacter* spp.

(This research was conducted by C. M. Callbeck in partial fulfillment of the requirements for a Ph.D. from the University of Bremen, 2017 [41].)

RESULTS

***Arcobacter* distribution in sulfidic Peru shelf waters.** The Peruvian shelf waters sampled onboard the RV *Meteor* Research Expedition M93 in February and early March

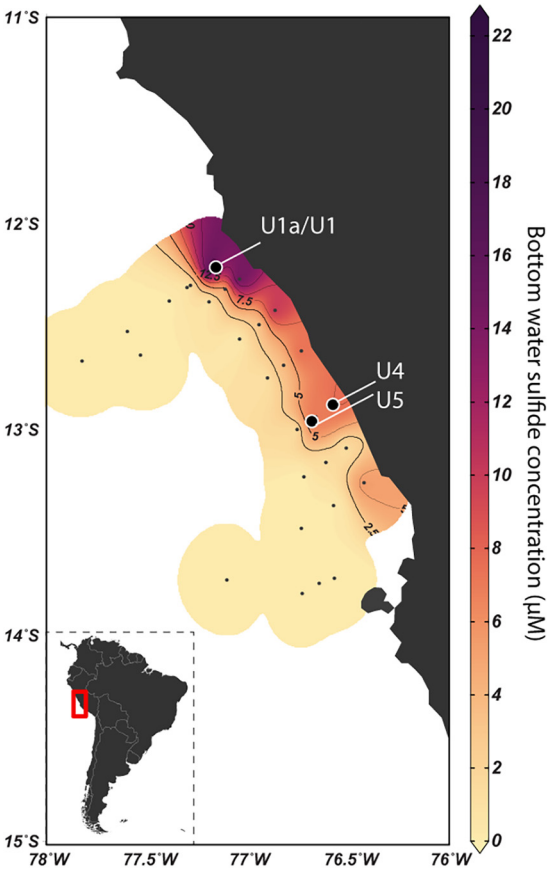

FIG 1 Sampling area off the coast of Peru and distribution of maximum dissolved sulfide in the shelf oxygen minimum zone. Maximum dissolved sulfide concentrations are shown for the sampling period from February to March 2013. Dots indicate water column sampling locations. Key sampling stations for microbiologic and biogeochemical studies are indicated with bold filled circles (see Table S1 in the supplemental material). Isolate PSE-93 was obtained from station U1a. Sulfide data were plotted with Ocean Data View software (R. Schlitzer, 2018 [62]).

2013 (Fig. 1; see also Table S1 in the supplemental material) were characterized by high chlorophyll concentrations and the extreme depletion of dissolved oxygen (<5 μM) below a depth of 10 m and nitrate below a depth of 30 m (27). Dissolved hydrogen sulfide was present in the anoxic waters that covered the entire near-shore Peruvian shelf between 12°S, 78.3°W and 13.3°S, 77°W (Fig. 1). Bottom water sulfide concentrations were typically 5 to 10 μM in the near-shore waters and at station U1a reached up to 23 μM (Fig. 1 and 2a). Potential denitrification rates at station U1a were the greatest in the redoxcline (6.5 ± 0.4 μM N day^{-1}) and decreased within the deeper sulfidic zone (0.9 ± 0.1 μM N day^{-1}). In contrast, dark carbon fixation rates remained constant at 2.8 ± 0.2 μM C day^{-1} throughout the redoxcline and into the deep sulfidic bottom waters. The nitrogen loss and carbon fixation rates measured on the shelf were similar to the rates in the Peru-Chile and Namibia shelf waters and indicated active chemolithoautotrophic activity, consistent with the findings of previous studies (6, 26, 28).

Bacteria belonging to the genus *Arcobacter*, as identified and enumerated using the fluorescent *in situ* hybridization (FISH) probe Arc94, were also detected throughout these near-shore, highly productive, sulfide-rich Peru upwelling bottom waters. At near-shore station U1a, the nitrate-sulfide redoxcline supported a large *Arcobacter* population, exceeding 10^6 cells ml^{-1}, that comprised 25% of the entire microbial community (Fig. 2b). At stations containing <10 μM dissolved sulfide in the bottom waters, *Arcobacter* was still present, but relative cell abundances were typically $<3\%$ of the microbial community, or below 10^5 cells ml^{-1} (Fig. S1). Offshore and in the absence

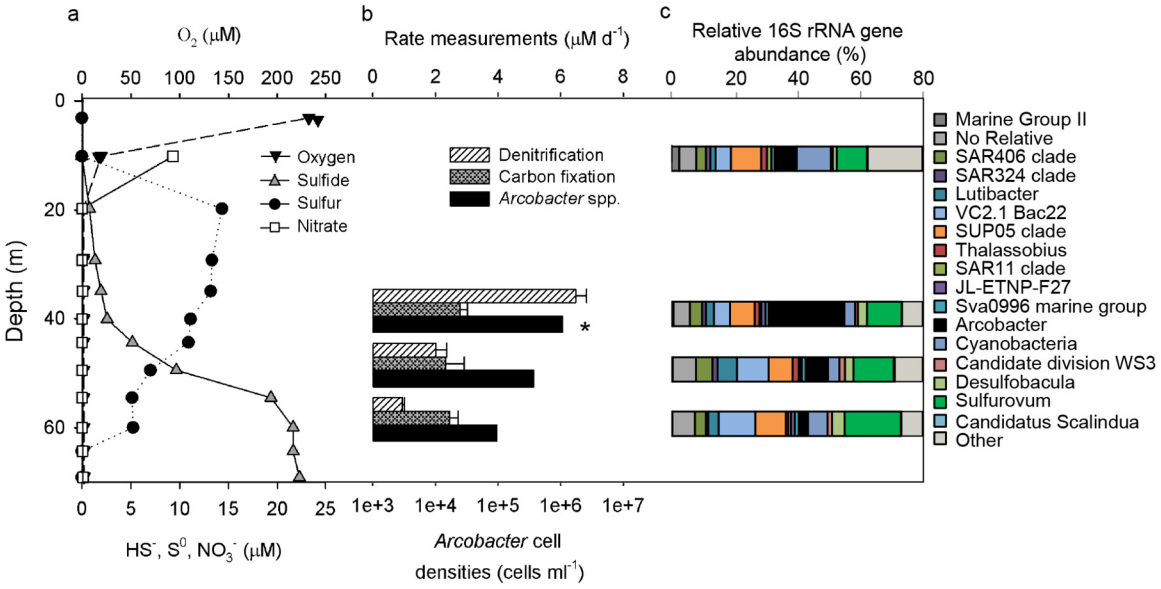

FIG 2 Depth distribution of concentrations, cell abundances, rates of dark carbon fixation and denitrification, as well as bacterial community diversity at station U1a (see Table S1 in the supplemental material). (a) Depth profiles of dissolved oxygen, sulfide, elemental sulfur, and nitrate. Nitrite concentrations were below the limit of detection throughout the water column, except at a 10-m depth (where they were up to 0.69 μM). (b) *Arcobacter* cell densities (Arc94 probe) and rates of dark carbon fixation and denitrification at 40-, 50-, and 60-m water depths are shown. Error bars represent the standard error. The asterisk indicates the depth from which the samples analyzed by nanoSIMS were collected. (c) Bacterial 16S rRNA gene diversity and relative abundances of key taxa; the top 18 most abundant taxa are shown.

of dissolved sulfide, *Arcobacter* abundances dropped below <0.1% of the microbial community, just at or below the limits of detection. Microbial 16S rRNA gene diversity analysis of station U1a redoxcline waters, using clone library and amplicon sequencing (pyrosequencing) techniques, identified common OMZ-occurring sulfide-oxidizing bacteria, such as the SUP05 (*U*"*Thioglobus perditus*, where the superscript "*U*" indicates an uncultivated taxon [27]) clade within the *Gammaproteobacteria*, as well as uncultured *Sulfurovum* and *Arcobacter* spp. within the *Epsilonproteobacteria* (Fig. 2c). *Arcobacter* abundances at station U1a, based on both catalyzed reporter deposition (CARD)-FISH cell counts and 16S rRNA gene abundances from amplicon pyrosequencing analysis (Fig. 2b and c), peaked at the middle of the broad redoxcline at 40 m, consistent with reports elsewhere of *Arcobacter* spp. occurring principally at oxic-sulfidic or nitrate-sulfidic redoxclines (4, 20, 42, 43).

Isolation and genome analysis of *Arcobacter* sp. strain PSE-93. We isolated an *Arcobacter* bacterium from station U1a under anaerobic conditions using natural seawater amended with sulfide and nitrate. The isolate, *Arcobacter* sp. strain PSE-93, was enriched from Peruvian seawater containing sulfide and nitrate by continuous transfers until it reached 90 to 95% purity, as checked with CARD-FISH using the Arc94 probe (Fig. S2). PSE-93 had a slightly elongated morphology (0.9 μm in length and 0.6 μm in width) that was comparable to the morphology of *Arcobacter* spp. observed *in situ*. DNA extraction of the enrichment culture, followed by sequencing by use of the Pacific Biosciences RS II technology (PacBio), assembly, and polishing, resulted in 256 contigs. After the removal of short contigs (<10 kbp) from the assembly, only one contig (84-fold average coverage) that was circularized remained, yielding the complete genome of PSE-93. Analysis by the CheckM method (44), based on 338 conserved marker genes, indicated that the genome of *Arcobacter* PSE-93 was complete (99.6%) and free of contamination (1.0%) or strain heterogeneity (0.0%). Summary genome statistics for *Arcobacter* PSE-93 are shown in Table S2.

The closed circular genome (2.8 Mbp in size with a 27.8% GC content and 2,697 predicted protein-coding genes) of PSE-93 revealed that it has the potential to reduce nitrate to N_2 via a complete denitrification pathway that includes periplasmic nitrate

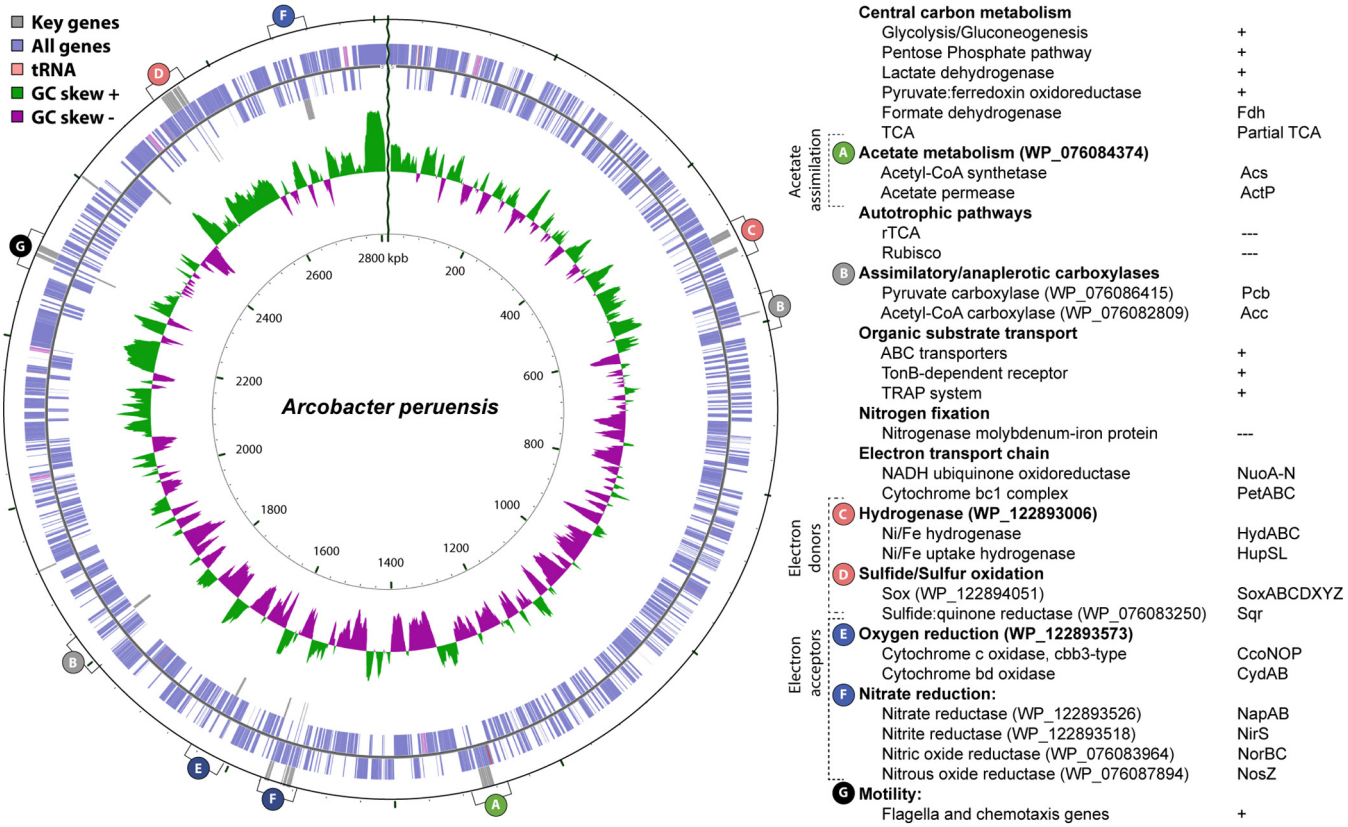

FIG 3 Central metabolism *of Arcobacter peruensis*. Identified genes are based on the RAST annotation. NCBI gene accession numbers associated with key genes discussed in the text are indicated. +, the genes were present; ---, the genes were not found in the genome; TCA, trichloroacetic acid; rTCA, reverse trichloroacetic acid; Rubisco, ribulose-1,5-bisphosphate carboxylase/oxygenase; TRAP, tripartite ATP-independent periplasmic transporter; ABC, ATP-binding cassette transporters.

reductase (*napAB*), cd_1-type nitrite reductase (*nirS*), nitric oxide reductase (*norBC*), and nitrous oxide reductase (*nosZ*) (Fig. 3). The presence of a cbb_3-type terminal oxidase (*fixNOQP*) implies that *Arcobacter* PSE-93 might be able to respire with oxygen. The identification of flagellum- and chemotaxis-associated genes in the PSE-93 genome indicated, furthermore, that *Arcobacter* might be able to position itself within the redoxcline according to the gradients of dissolved sulfide and nitrate. A gene encoding a protein with a rhodanese-like domain that may act to shuttle zerovalent sulfur in between redox centers during sulfur metabolism was found (45). The *Arcobacter* PSE-93 genome contained a complete periplasmic sulfide oxidation Sox pathway (*soxABCDXYZ*) and a sulfide-quinone reductase gene (*sqr*) that allows for the oxidation of various reduced sulfur compounds (including sulfide, sulfur, and thiosulfate) to sulfate. The presence of *soxCD* is consistent with a lack of internal elemental sulfur storage, as missing *soxCD* genes have been shown in other sulfide oxidizers to be correlated with intracellular sulfur storage (46). Sulfur reduction genes, such as those for polysulfide reductase, tetrathionate reductase, and sulfide hydrogenases, some of which have been identified in *A. anaerophilus* (10), were absent from the *Arcobacter* PSE-93 genome.

Key genes associated with autotrophic CO_2 fixation (e.g., ribulose-1,5-bisphosphate carboxylase/oxygenase [Rubisco] and succinyl coenzyme A [CoA] synthetase reverse trichloroacetic acid [rTCA]), which are frequently identified in sulfide-oxidizing bacteria and in other autotrophic members of the genus *Arcobacter* (1, 9, 10), were not found in the *Arcobacter* PSE-93 genome (Fig. 3), nor were genes responsible for nitrogen (N_2) fixation present. Instead, genes encoding organic matter-dependent carboxylases involved in acetate and propionate assimilation were detected, as were genes encoding carboxylases involved in fatty acid biosynthesis and anaplerotic reactions. Genes en-

coding organic compound transporters, e.g., TonB-dependent receptors and TRAP (tripartite ATP-independent periplasmic transporter)-type C_4 transport systems, including acetate permeases and ABC transporters associated with acetate and glucose metabolisms, were also detected in the genome. Alternative electron donors may also include formate (formate dehydrogenase) and hydrogen, for example, Ni/Fe hydrogenases, which have also been identified in marine *Arcobacter* species associated with unicellular protists (18).

The genome of *Arcobacter* PSE-93 contained six complete sets of rRNA genes (16S-23S-5S). The 16S rRNA gene sequences were almost identical and shared up to 7 mismatches (>99.53% identity). Multiple copies of rRNA genes appear to be a common feature of microorganisms within the genus *Arcobacter* (44) and might offer a competitive advantage because they confer a higher growth rate or competitive fitness (47). Furthermore, multiple copies of rRNA genes can lead to an overestimation of *Arcobacter* abundances in the environment and should be considered when interpreting 16S rRNA gene amplicon sequencing data.

Physiology of the PSE-93 isolate. We tested the ability of isolates of *Arcobacter* PSE-93 to oxidize sulfide and reduce nitrate on various carbon substrates under anoxic conditions. In all subsequent physiology experiments, we used plate-grown colonies (colonies grown on PY-BROTH medium [DSMZ, Germany]) obtained from the isolate described above, which were then transferred to axenic liquid medium. The identity and purity of the transferred *Arcobacter* PSE-93 colonies were verified by full 16S rRNA sequencing. Enough dissolved sulfide was amended to reduce all added nitrate to N_2, assuming the complete oxidation of sulfide to sulfate. In natural seawater experiments (in North Sea seawater [saNS] medium) under autotrophic conditions (i.e., in the absence of added organic carbon substrate), PSE-93 showed slightly enhanced rates of sulfide oxidation ($1.29 \pm 0.26\ \mu M\ h^{-1}$) and nitrate reduction ($1.00 \pm 0.04\ \mu M\ h^{-1}$) (Fig. 4a and d; Table 1). *Arcobacter* PSE-93 cell densities never exceeded 9×10^4 cells ml^{-1}, and the cells exhibited negligible to nondetectable [^{13}C]bicarbonate assimilation rates under these autotrophic conditions (Fig. 4d). Similarly, using synthetic seawater (Sas) medium under autotrophic conditions, cell numbers also never reached more than 3×10^5 cells ml^{-1} (Fig. S3). In both experiments, sulfide consumption occurred, and nitrate reduction rates were detectable (Fig. 4a and d; Table 1; Fig. S3). Neither sulfide nor nitrate was fully consumed; roughly half of the nitrate was reduced to N_2, while the rest of the added nitrate was reduced only to nitrite.

Complete nitrate reduction ($>4.1\ \mu M\ h^{-1}$) to dinitrogen as well as enhanced sulfide oxidation ($>1.5\ \mu M\ h^{-1}$) did ensue when PSE-93 was grown heterotrophically on glucose, yeast extract, or acetate (Table 1). The nitrite that formed as an intermediate was completely reduced to N_2 by the end of the experiment (Fig. 4b). Growth on acetate yielded the highest rates of sulfide oxidation ($6.6 \pm 0.67\ \mu M\ h^{-1}$) and nitrate reduction ($6.2 \pm 1.69\ \mu M\ h^{-1}$) for PSE-93 (Fig. 4b and d; Table 1). ^{13}C-labeled acetate incorporation during growth on nitrate, dissolved sulfide, and acetate showed that acetate was assimilated into PSE-93 biomass at a rate of 1.55 ± 0.19 fmol C $cell^{-1}$ day^{-1}. Growth under these conditions yielded high cell densities of 4×10^6 cells ml^{-1} with a doubling rate of 1.4 to 1.8 per day (calculated from cell abundances and ^{13}C assimilation rates). *Arcobacter* PSE-93 was also able to grow heterotrophically, coupling acetate oxidation to nitrate reduction (Fig. 4c and d); however, the nitrate reduction ($1.3 \pm 0.22\ \mu M\ h^{-1}$) and acetate assimilation (0.38 ± 0.06 fmol C $cell^{-1}$ day^{-1}) rates were over 4-fold lower, and the calculated doublings per day (0.8 to 1.0) were nearly 2-fold lower than the rate of PSE-93 growth on dissolved sulfide, nitrate, and acetate (Fig. 4c and d; Table 1). These experiments demonstrated that the Peru upwelling *Arcobacter* PSE-93 strain is an obligate heterotroph capable of chemolithoheterotrophic and chemoorganoheterotrophic growth. More importantly, *Arcobacter* PSE-93 could couple sulfide oxidation to complete denitrification when low-molecular-weight organic carbon was made available for cell biomass synthesis.

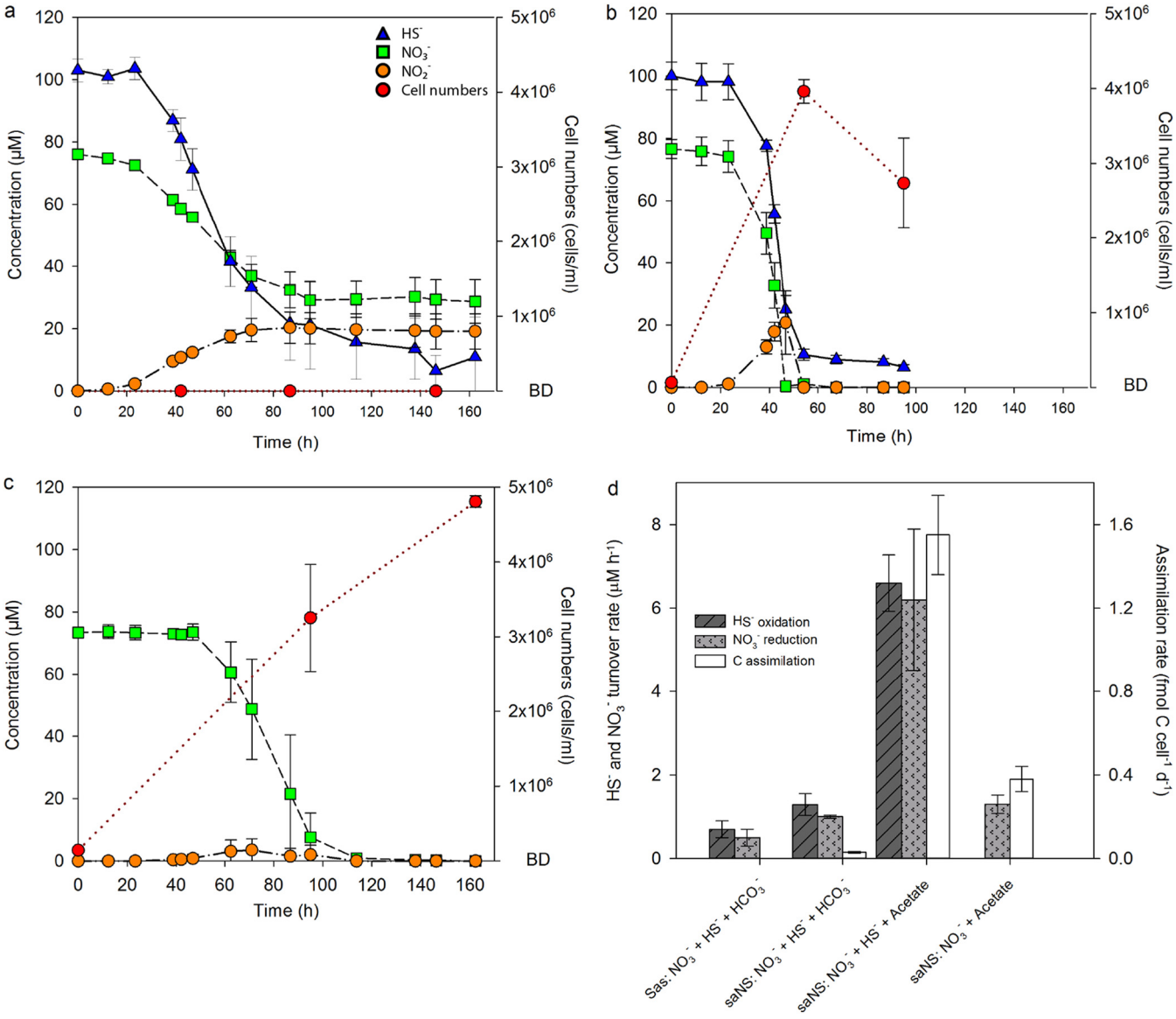

FIG 4 *Arcobacter peruensis* activity and growth. Experiments were performed in saNS medium with sulfide, nitrate, and [^{13}C]bicarbonate (a), sulfide, nitrate, and [^{13}C]acetate (b), and nitrate and [^{13}C]acetate (c). (d) Rates of C assimilation based on [^{13}C]bicarbonate and [^{13}C]acetate single-cell uptake determinations. Error bars represent the standard deviations from triplicate incubation experiments. BD, below the limit of detection ($<9 \times 10^4$ cells ml^{-1}).

Phylogeny of *Arcobacter* PSE-93. PSE-93 formed a distinct clade that was different with respect to the four recently defined *Arcobacter* type strain clusters (48). The closest type strains to PSE-93 were in cluster 2, which contained *A. venerupis*, *A. suis*, *A. ellisii*, *A. cloacae*, and *A. defluvii* (Fig. 5). To place the PSE-93 identity in relation to the *Arcobacter* diversity in the Peruvian upwelling, we analyzed the 16S rRNA genes recovered from station U1a. From the nearly full-length 16S rRNA amplicon sequences obtained from clone library preparations at station U1a, we identified two Peruvian *Arcobacter* clones. ETSP (Eastern Tropical South Pacific) clone 3 and ESTP clone 5 formed two separate phylogenetic branches (Fig. 5). Sequences affiliated with ETSP clone 5 contained *Arcobacter* members capable of both CO_2 fixation (e.g., *A. sulfidicus* and *A. nitrofigilis*) and acetate assimilation. In contrast, ETSP clone 3 and the nearby affiliated PSE-93 lineage contained, to the best of our knowledge, only members capable of heterotrophic growth.

Arcobacter PSE-93 was most closely affiliated with the *Arcobacter* clade that contained ETSP clone 3 (96.1% 16S rRNA gene identity). Within this clade, the sequence of

TABLE 1 *Arcobacter* PSE-93 sulfide oxidation and nitrate reduction activity in amendment experiments[a]

Expt	Activity (μM h^{-1})		Estimated no. of doublings/day
	Sulfide oxidation	Nitrate reduction	
Sas medium with NO_3^- + HS^- + HCO_3^-	0.70 ± 0.20	0.50 ± 0.20	0.86
saNS medium with NO_3^- + HS^- + HCO_3^-	1.29 ± 0.26	1.00 ± 0.04	BD
saNS medium with NO_3^- + HS^- + glucose	1.50	4.1	ND
saNS medium with NO_3^- + HS^- + yeast extract	2.60	4.7	ND
saNS medium with NO_3^- + HS^- + acetate	6.60 ± 0.67	6.20 ± 1.69	1.82
saNS medium with NO_3^- + acetate		1.3 ± 0.22	0.78

[a]Experiments were performed in synthetic seawater (Sas) medium or North Sea seawater (saNS) medium, as indicated. The sulfide and nitrate turnover rates shown here were determined from the change in the substrate concentration divided by time (Fig. 4). Carbon assimilation rates are reported in the text. The estimated number of doublings per day is based on the ^{13}C uptake rates. BD, below the limit of detection; ND, not determined.

PSE-93 was most closely related to a sequence recovered from the North Sea, that of *Arcobacter* sp. strain KT0913 (49), and nearly identical to that of *Arcobacter* sp. strain LPB0137 (the 16S rRNA gene from an environmental Korean strain). *Arcobacter* strain KT0913 shares a 16S rRNA gene identity value with PSE-93 above the species level (98.8%) (49); however, confirmation by comparison of the average nucleotide identity (ANI) values awaits the availability of the genome sequence of KT0913. Although *Arcobacter* PSE-93 enriched in our incubations was not identical to ETSP clone 3 or 5, our phylogenetic analysis suggests that PSE-93 is a close relative of ETSP clone 3, one of the most abundant Peruvian upwelling *Arcobacter* members. Additionally, the *Arcobacter* 16S rRNA genes recovered from 454 pyrosequencing (~450 bp in length) were closely related to the clone library 16S rRNA genes, as well as to the 16S rRNA gene of the *Arcobacter* PSE-93 isolate (e.g., ETSP pyrotags 4, 5, and 6).

***In situ* single-cell analysis.** From isotope labeling experiments performed on samples obtained during RV *Meteor* Research Expedition M93 in Peru, we used nanoscale secondary ion mass spectrometry (nanoSIMS) to obtain single-cell measurements of the *Arcobacter* composition and the uptake of CO_2 in the *in situ* population (Fig. 6). The analysis of single-cell $^{13}CO_2$ assimilation rates showed that *Arcobacter* fixed 0.03 ± 0.01 fmol CO_2 $cell^{-1}$ day^{-1}. This rate was significantly lower than the measured CO_2 assimilation rates for *Gammaproteobacteria* clade SUP05 and other *Epsilonproteobacteria* (e.g., *Sulfurovum* spp.) of 0.19 ± 0.02 and 0.72 ± 0.03 fmol C $cell^{-1}$ day^{-1}, respectively (analysis of variance [ANOVA], degrees of freedom [df] = 2, $P < 0.001$ [considered a significant difference]; Fig. 6b). *Arcobacter* bacteria thus contributed to less than 1% of the overall dark CO_2 fixation at station U1a, despite the large abundance of *Arcobacter* (25% of the total microbial community), whereas the *Gamma-* and *Epsilonproteobacteria* accounted for nearly one-quarter of the total dark carbon fixation rates at station U1a, consistent with their abundances (Table S3). The *Arcobacter* spp. present in the Peru upwelling waters also differentiated themselves from the SUP05 clade and other *Epsilonproteobacteria*, in that *Arcobacter* exhibited significantly lower sulfur contents than these other groups of sulfide-oxidizing bacteria (Fig. 6c).

DISCUSSION

The genotypic and physiologic characterizations of the isolated *Arcobacter* PSE-93 strain demonstrate that we have isolated a new *Arcobacter* species that we name *Arcobacter peruensis*. Both the chemolithoheterotrophic genotype and the physiology of *A. peruensis* suggest that it can thrive in the sulfide- and organic matter-rich environment in coastal Peru upwelling waters, where nitrate is supplied as an alternate electron acceptor. Our experiments employing environmentally relevant concentrations of substrates demonstrated that *A. peruensis* grows best on a combination of hydrogen sulfide, nitrate, and acetate. It appears to be uniquely suited to an environment where nitrate or microaerophilic concentrations of dissolved oxygen are present and where the fluxes of small dissolved organic compounds (e.g., acetate) and sulfide are great enough to enhance growth. The obligate organotroph *A. peruensis* thus differs from other environmentally relevant *Arcobacter* species, which are either facultative hetero-

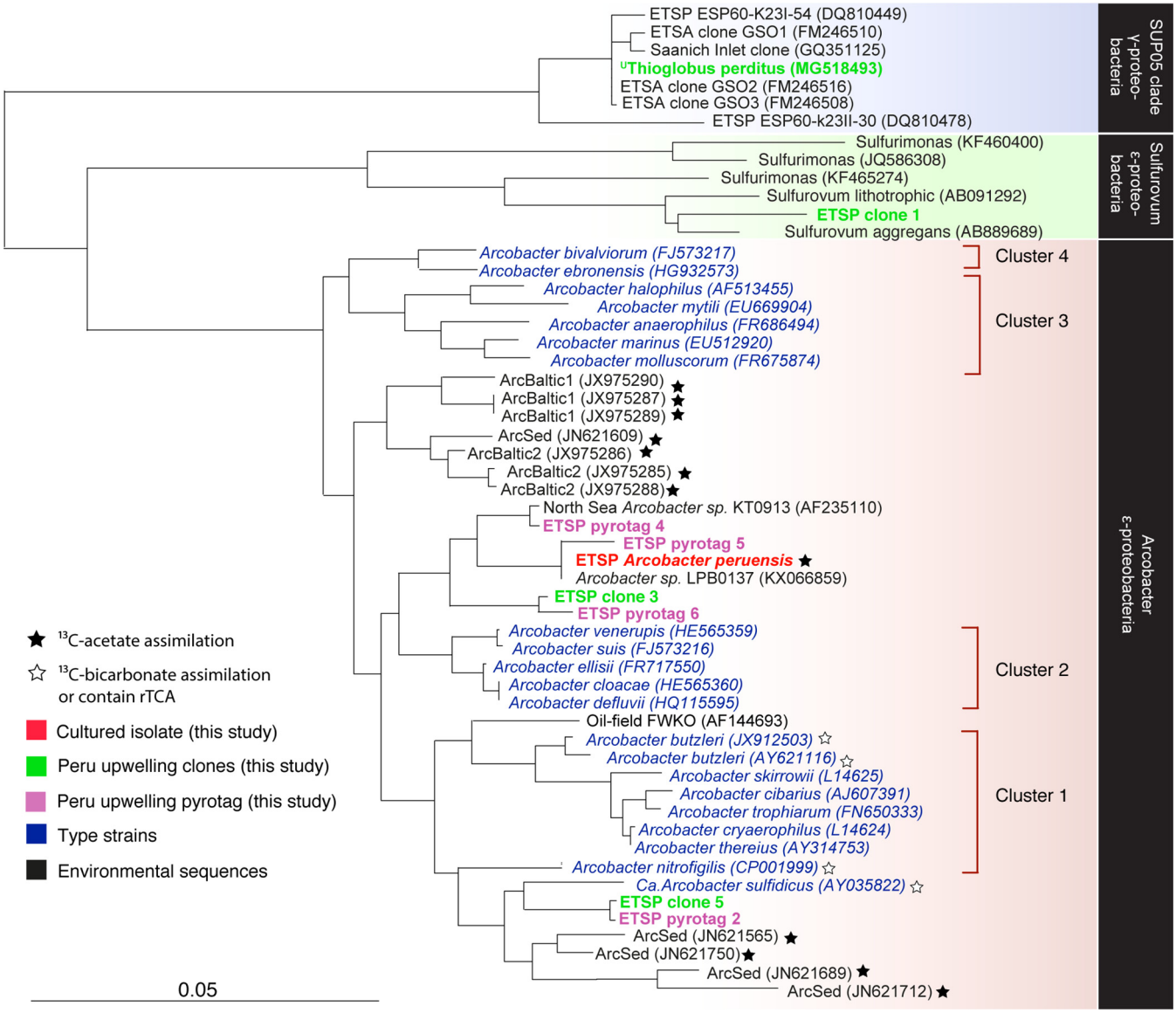

FIG 5 Phylogeny of 16S rRNA genes of key sulfide-oxidizing bacteria recovered from Peruvian shelf waters. The unrooted consensus tree is based on the neighbor-joining, parsimony, and RAxML methods applying various *Epsilonproteobacteria* filters. The *Arcobacter* type strains (in blue) are organized into four distinct clusters, as defined previously (48). Included are partial and nearly full-length 16S rRNA sequences recovered from sulfidic station U1a (green; Fig. 1; see also Fig. S1 in the supplemental material) and the 16S rRNA gene of the *Arcobacter peruensis* (PSE-93) isolate enriched from sulfidic station U1a (red). *Arcobacter* sequences recovered from [^{13}C]acetate RNA-stable isotope assimilation experiments are indicated by black stars (5, 8); conversely, strains capable of autotrophic carbon fixation are indicated by open stars (1, 9, 78). The scale bar represents the substitution rate per site.

trophs and which can also grow autotrophically, such as *A. anaerophilus* (10), or which are strict autotrophs, such as *A. sulfidicus* (1). The lack of genes for autotrophic CO_2 fixation pathways and the presence of genes for organic carbon-dependent carboxylases in the genome indicate that the very low measured rates of CO_2 assimilation might be attributable to anaplerotic CO_2 uptake during organotrophy. In addition to being an obligate organotroph, *A. peruensis*, unlike *A. anaerophilus* and *A. nitrofigilis*, has no nitrogen fixation genes and therefore lacks the ability to fix N_2 for growth.

In contrast to other *Arcobacter* species that can reduce nitrate to ammonium (e.g., *A. butzleri* and *A. nitrofigilis*) (11, 50), *A. peruensis* reduces nitrate to dinitrogen. The genes for a complete denitrification pathway are present in the genome of *A. peruensis* (Fig. 3), and the presence of this pathway was confirmed by the ^{15}N labeling experiments. Complete denitrification by *A. peruensis* contrasts with the denitrification ability

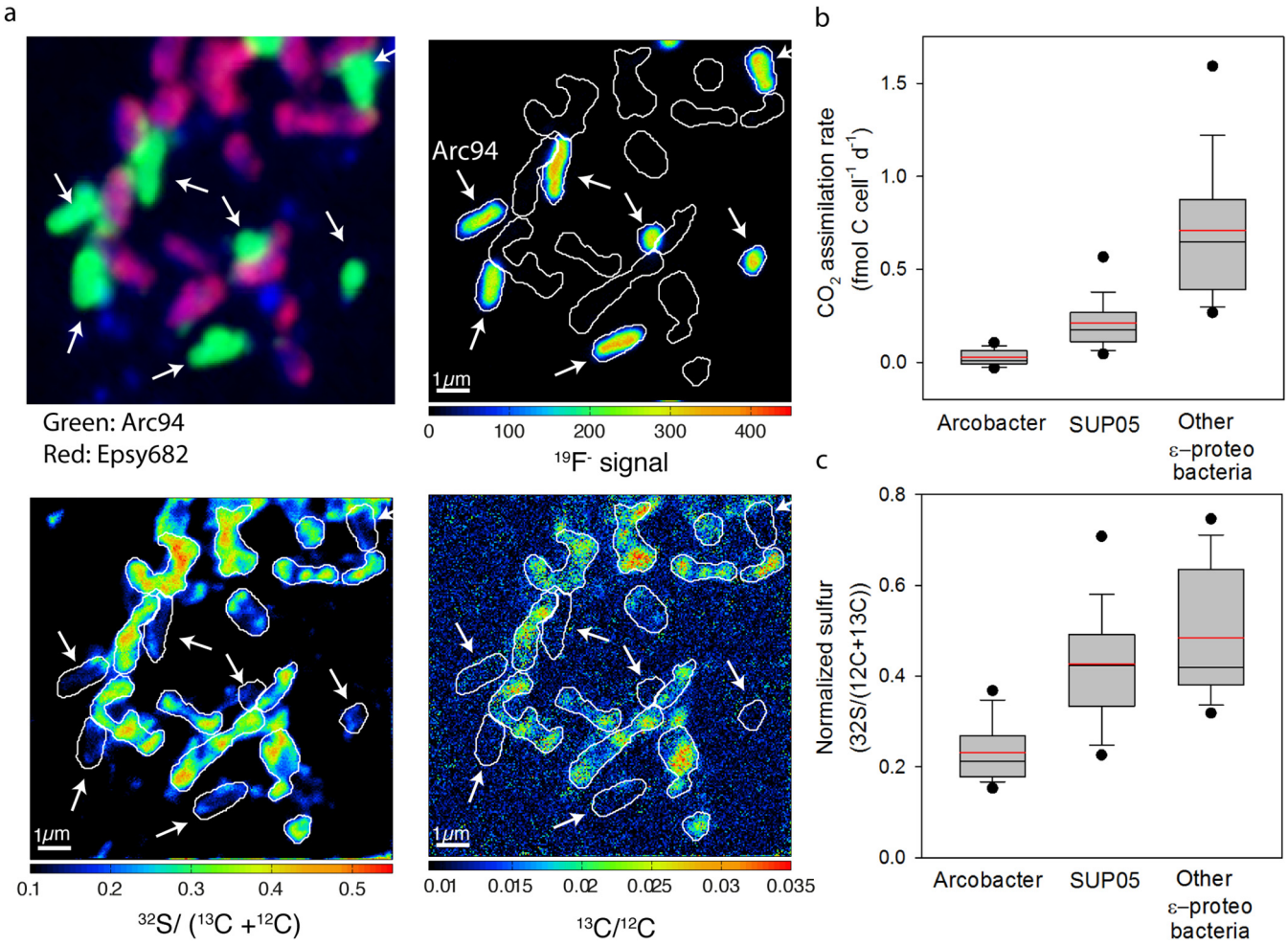

FIG 6 *Arcobacter* single-cell activity and sulfur content at Peruvian upwelling station U1a (60-m depth). (a) The composite images show the CARD-FISH image and the single-cell isotope ratios. In the CARD-FISH image, cells in green and red are hybridized with the Arc94 and Epsy682 probes, respectively. The ^{19}F signal indicates cells that hybridized with the Arc94 probe (also indicated by the white arrows). (b and c) The single-cell $H[^{13}C]CO_3^-$ assimilation rates (b) and cell sulfur contents (c) of *Arcobacter*, SUP05, and other *Epsilonproteobacteria* (excluding *Arcobacter*) are shown. The average (red line) and median (black line) as well as the 5th and 95th percentiles (closed circles) are indicated. Error bars represent the standard deviation. The numbers of cells analyzed by nanoSIMS were 58, 37, and 107 for *Epsilonproteobacteria*, *Arcobacter*, and SUP05, respectively. Note that data related to SUP05 (including the SUP05 single-cell assimilation rates and sulfur content) are presented elsewhere (27).

of *A. anaerophilus*, which is also capable of reducing nitrate to nitrite but lacks the *nir* and *nrf* genes and, thus, the ability to reduce nitrite and nitric oxide. On the other hand, *A. anaerophilus* can use reduced sulfur species, such as tetrathionate and zerovalent sulfur (in the form of elemental sulfur or polysulfides), to oxidize organic compounds. Genomic analysis indicates that *A. peruensis* does not appear to have the capacity to use intermediate-oxidation-state sulfur compounds as an electron acceptor. It is true that the *A. peruensis* isolate can also grow heterotrophically on acetate in the absence of sulfide, but it does so only poorly, as the estimated doublings per day are 2-fold lower than those in the presence of dissolved sulfide (Table 1). Our experiments suggest that *A. peruensis* grows best by coupling dissimilatory nitrate reduction to dinitrogen with the oxidation of dissolved sulfide (Fig. 4) and that environmental levels of sulfide, nitrate, and acetate could sustain the abundances of *Arcobacter* cells observed *in situ* (Fig. 2b).

The low rates of CO_2 fixation determined by single-cell analysis of the *in situ* *Arcobacter* population (Fig. 6) are consistent with the conclusion that chemolithoheterotrophic *A. peruensis* probably dominates the *in situ Arcobacter* community. The rate of *Arcobacter* CO_2-based growth, as measured by *in situ* single-cell ^{13}C uptake, would

be far too low (doubling once per 100 days) to support the large cell densities of *Arcobacter* observed *in situ*, if it were an autotroph. We ascribe the low per cell rates of CO_2 fixation to anaplerotic reactions. In contrast, *^U^T. perditus* (SUP05) and *Epsilonproteobacteria* show active autotrophy *in situ* (27) (Fig. 6) and contribute substantially (11% to 51%) to the rates of dark carbon fixation on the Peru shelf (see Table S2 in the supplemental material).

Acetate, a short-chain fatty acid produced during the degradation of organic matter via fermentation, could support *Arcobacter* growth in the Peruvian OMZ waters. Permanently sulfidic marine basins exhibit not only elevated rates of dark carbon fixation but also high rates of both acetate production and acetate assimilation (0.05 to 0.5 μM day^{-1}) (51). Acetate assimilation has been suggested to provide an important source of carbon for microbial growth on the highly productive northern Gulf of Mexico shelf (52). *A. peruensis* could assimilate acetate by converting it to acetyl-CoA using the combination of the high-affinity acetate permease (K_m = 5.4 μM) and the acetyl-CoA synthetase (53, 54) (Fig. 3). Acetyl-CoA is a key precursor molecule for various biosynthesis pathways (55). Interestingly, the *Arcobacter* strain isolated and described here was initially enriched on Peru OMZ shelf water without the addition of extra organic substrates, suggesting that *A. peruensis* is very efficient at exploiting the residual dissolved organic pool in the Peru OMZ. The concentrations of dissolved organic matter in surface and benthic zone-influenced bottom waters of the shallow Peruvian OMZ shelf are high and in the range of 80 to 100 μmol liter^{-1} (56). Furthermore, other studies have indicated that *Arcobacter* species may be capable of assimilating acetate under sulfidic conditions within sediments and at redoxclines (3, 8).

Chemolithoheterotrophic growth may confer energetic advantages over a chemolithoautotrophic physiology in an organic matter-rich environment. For pyruvate, a key building block in biosynthesis, autotrophic CO_2 fixation requires between 0.6 and 2.3 mol ATP per mol of pyruvate formed, while acetate assimilation requires only 0.5 mol ATP per mol of pyruvate formed (57). From the nanoSIMS-derived PSE-93 culture single-cell acetate assimilation rates (1.55 fmol C cell^{-1} day^{-1}) obtained during experiments under sulfide-oxidizing, denitrifying conditions, we calculated an assimilation factor of 3.1 mol C per mol H_2S oxidized. This rate of acetate carbon assimilation exceeds the rates of CO_2 assimilation reported for cultivated chemolithoautotrophic sulfide-oxidizing bacteria, which range from 0.35 to 0.58 mol C assimilated per mol H_2S oxidized (58–60). The lower energy constraints of *A. peruensis* may enable *A. peruensis* (and, presumably, other sulfide-oxidizing chemolithoheterotrophic bacteria) to outcompete sulfide-oxidizing chemolithoautotrophs (e.g., SUP05 bacteria) when the production or flux of small organic compounds is sufficient. Thus, *A. peruensis* is most likely to bloom under highly sulfidic and organic matter-rich conditions, as observed in this study off the coast of Peru, and at other coastal, sulfidic environments, such as off the coast of Namibia (6).

A chemolithoheterotrophic physiology is not without drawbacks. The requirement for labile organic matter, in addition to sulfide and nitrate, places *A. peruensis* at a competitive disadvantage alongside chemolithoautotrophic bacteria that generate biomass (i.e., via CO_2 fixation) independently of organic matter availability. In addition, compared to other co-occurring sulfide-oxidizing bacteria (e.g., SUP05), *A. peruensis* appears to lack the capacity to store intracellular sulfur. Genomic data showed the presence of the *soxCD* genes, which is often correlated with a lack of intracellular sulfur storage in sulfide oxidizers (46). NanoSIMS analysis of individual cells showed, moreover, that Peruvian OMZ *Arcobacter* spp. were significantly lower in sulfur content (ANOVA, df = 2, $P < 0.001$) than SUP05 and non-*Arcobacter Epsilonproteobacteria* cells (Fig. 4a and b). In contrast, SUP05 bacteria, which co-occur with *Arcobacter* in the sulfidic shelf waters, continue to denitrify using stored intracellular elemental sulfur and are, as a result of this ecophysiology, more broadly distributed within the Peru upwelling OMZ (27). In contrast, the *Arcobacter* dependency on sulfide and organic matter for growth ultimately constrains its distribution to sulfidic and highly productive shelf waters.

The metabolic flexibility inherent to the *Arcobacter* genus has enabled *Arcobacter* strains similar to *A. peruensis* to gain a foothold in a marine redox transition zone that is often assumed to be dominated by chemolithoautotrophs (6, 26, 28, 35, 37, 38). Despite its apparent restriction to sulfidic, eutrophic shelf systems, chemolithoheterotrophic metabolism, such as that exhibited by *A. peruensis*, may play an important role in nitrogen and sulfur cycling in environments similar to those on the Peru shelf, especially as hypoxic, sulfidic coastal regions expand (32). Organisms similar to the Peru upwelling *A. peruensis* bacterium may be more widely spread, as indicated by the very close similarity of a Korean environmental strain (LPB0137). How much these and similar *Arcobacter* species eventually contribute to sulfide oxidation and nitrogen loss through denitrification in increasingly eutrophic marine coastal ecosystems remains to be explored.

Description of *Arcobacter peruensis* sp. nov. *A. peruensis* type strains: PSE-93, LMG 31510. Etymology: pe.ru.en'sis. N.L. masc. adj. *peruensis*, pertaining to Peru. Locality: isolated from coastal, sulfidic Peruvian shelf waters at 12.23°S, 77.18°W. Properties: Gram-negative, slightly elongated rods (0.9 μm in length and 0.6 μm in width). It grows chemolithoheterotrophically in sulfide-, nitrate-, and organic matter-rich environments in coastal upwelling water. It grows best by coupling dissimilatory nitrate reduction to dinitrogen to the oxidation of dissolved sulfide. Alternatively, heterotrophic growth on acetate in the absence of sulfide occurs, albeit at much slower doubling times. It grows aerobically on PY-BROTH medium (DSMZ, Germany) supplemented with 200 μM KH_2PO_4, 10 mM $MgSO_4{\cdot}7H_2O$, 5 mM HEPES at a final pH of 7.8 and solidified with Bacto agar (1%, wt/vol). The median GC content of the type strain is 27.4 mol%.

MATERIALS AND METHODS

Sampling and water chemistry. Peru upwelling waters (12°S, 78.5°W and 13.5°S, 77°W) were sampled from 8 February to 4 March 2013 onboard the RV *Meteor* (Research Expedition M93; Fig. 1; see also Table S1 in the supplemental material). All seawater samples for this study were collected at an approximately 5-m resolution to within 5 m of the seafloor using a conductivity-temperature-depth (CTD) rosette equipped with 10-liter Niskin bottles. Oxygen was monitored with a Seabird sensor and calibrated against Niskin bottle samples by Winkler titration. Collected seawater nitrate and nitrite concentrations were determined with a QuAAtro autoanalyzer (Seal Analytical, UK) with precisions of $\pm$0.1 μM. Sulfide concentrations were determined onboard as described by Cline (61) using 4 ml of seawater. The sulfide data in Fig. 1 were plotted with Ocean Data View software (62). For the determination of water column elemental sulfur, 50-ml samples of seawater were sampled using anaerobic techniques, fixed with 100 μl $ZnCl_2$ (20%, wt/wt), and stored at $-$20°C. Elemental sulfur was extracted from the Zn-fixed samples using a chloroform-methanol procedure (63) and measured on a Waters Acquity H-class (Waters, Japan) ultra-high-pressure liquid chromatography (UPLC) system (1.7-μm-particle-size, 2.1- by 50-mm column with a methanol eluent at a flow rate of 0.4 ml min^{-1}; Acquity UPLC BEH C_{18}) equipped with a Waters photometric diode array detector (the absorbance wavelength was set to 265 nm, with the limit of detection being 50 nM). In this procedure, elemental sulfur can derive from suspended elemental sulfur, from elemental sulfur deposited on or within cells, or from the decomposition of dissolved polysulfides (63).

Microbial diversity analysis. One to 2 liters of seawater was collected on polycarbonate filters (0.2-μm pore size; Millipore, Germany) for genomic DNA extraction. Genomic DNA was extracted using a Qiagen AllPrep DNA/RNA kit) and quantified spectrophotometrically by use of a NanoDrop spectrophotometer (Thermo Scientific). Universal bacterial barcoded PCR primers (primers Bakt341F [CCTACG GGNGGCWGCAG] and 805R [GACTACHVGGGTATCTAATCC], targeting the V3-V4 regions [59]) were used to generate amplicons for 454 pyrosequencing (454 FLX+ Titanium chemistry; Max Planck Genome Center, Cologne, Germany [https://mpgc.mpipz.mpg.de/home/]). The PCR conditions were initial denaturation at 95°C for 5 min, followed by 25 cycles of 95°C for 40 s, 55°C for 2 min, and 72°C for 1 min and a final extension of 72°C for 7 min, with a ramp rate of 3°C s^{-1}. The PCR products were purified using a QIAquick PCR purification kit (Qiagen, Hilden, Germany). The recovered 16S rRNA sequences were trimmed to remove the primer adaptors before submission to the SILVAngs pipeline, which provided automated alignments, quality management, dereplication, and taxonomic classification (60).

The microbial diversity at station U1a was also analyzed by clone library sequencing, which produced nearly full-length 16S rRNA gene sequences. The clone library preparation procedure, including raw read quality controls and taxonomic classification using ARB software, was performed by a method similar to that described by Callbeck et al. (27). Universal bacterial primers GM3f (5′-AGA GTT TGA TCM TGG C-3′) and GM4r (5′-TAC CTT GTT ACG ACT T-3′) were used to generate 16S rRNA PCR amplicons from DNA samples taken at station U1a. The PCR conditions were initial denaturation at 95°C for 5 min, followed by 25 cycles of 95°C for 1 min, 50°C for 1 min, and 72°C for 2 min and a final extension of 72°C for 10 min, with a ramp rate of 3°C s^{-1}. DNA was visualized by gel electrophoresis. The 16S rRNA PCR amplicons were purified and then ligated into a TOPO TA vector (Invitrogen). *Escherichia coli* clones were picked and

screened for the vector insert by PCR. The plasmids were extracted from vector-positive colonies (using a plasmid extraction kit [MoBio]), and then the plasmid vector was PCR amplified using forward and reverse M13 primers (primers M13f [5′-CCC AGT CAC GAC GTT GTA AAA CG-3′] and M13r [5′- AGC GGA TAA CAA TTT CAC ACA GG-3′]). The PCR products were purified using Sephadex (G-50 Superfine; Amersham Bioscience) and then sequenced (Sanger sequencing with a BigDye kit; Applied Biosystems). Raw sequence data were quality controlled, and vector ends were trimmed and then assembled into nearly full-length 16S rRNA contigs using Sequencher (version 4.6) software (Gene Codes Corporation, Ann Arbor, MI). The nearly full-length and partial 16S rRNA sequences recovered from the clone library preparations and from pyrosequencing were aligned by use of the SINA aligner (64) and then imported into the SILVAref115 curated 16S rRNA reference database (65) using ARB software (66). A consensus 16S rRNA gene tree of neighbor-joining (distance matrix), parsimony (Phylip DNApars program), and maximum likelihood (RAxML, version 7, software) phylogenetic trees applying various epsilonproteobacterial filters was calculated from the nearly full-length sequences (67). Partial 16S rRNA genes were added to the consensus tree using RAxML (version 7) software, applying an epsilonproteobacterial filter.

Cell identification and enumeration. Seawater samples collected from Niskin bottles were filtered over polycarbonate filters (0.2-μm pore size; Millipore, Germany) for analysis of cell abundances and identification. The filters were fixed in paraformaldehyde (final concentration, 1 to 2% [wt/vol]) for 12 h at 4°C prior to filtration. Catalyzed reporter deposition (CARD)-FISH analysis was performed using probes targeting *Arcobacter* and general *Epsilonproteobacteria*: Arc94 (5′-TTAGCATCCCCGCTTCGA-3′) (68) and Epsy682 (5′-CGGATTTTACCCCTACACM-3′) (43). The Arc94 and Epsy682 probes were incubated in 20% formamide containing hybridization buffer at 46°C for 3 h. The total microbial community was stained with 4′,6-diamidino-2-phenylindole (DAPI), and together, DAPI-stained and Arc94- and Epsy682-hybridized cells were visualized and quantified using epifluorescence microscopy. Hybridized cells in 10 fields of view and up to 1,000 DAPI-stained cells were counted. Negative and positive controls were performed using the NON338 and EUB3381-III probes, respectively, as described previously (69).

^{15}N- and ^{13}C-labeled incubation experiments. Isotope labeling experiments to determine the rates of nitrate reduction (^{15}N labeling) and CO_2 fixation (^{13}C labeling) were performed as described previously (70). Briefly, denitrification, as well as bulk and single-cell carbon fixation rates, were determined from 12-ml Exetainer incubation experiments, as follows: in experiment 1, $^{15}NO_3^-$ plus $H^{13}CO_3^-$; in experiment 2, $^{15}NO_2^-$ plus $^{14}NH_4^+$ plus $H^{13}CO_3^-$; and in experiment 3, $^{15}NH_4^+$ plus $^{14}NO_2^-$ and $H^{13}CO_3^-$. The concentrations of labeled substrates were 25 μM, 5 μM, and 5 μM for NO_3-, NO_2-, and NH_4^+, respectively. Isotopic ratios of $^{15}N^{15}N$, $^{15}N^{14}N$, and $^{14}N^{14}N$ nitrogen gas were measured on a gas chromatography (GC) isotope-ratio mass spectrometer (IRMS) (VG Optima, Manchester, UK), while bulk carbon fixation rates were measured separately in ^{13}C incubation experiments performed in gas-tight 4.5-liter bottles (26). The $^{13}C/^{12}C$ isotope ratio was measured on an element analyzer (EA) IRMS (FlashEA 1112 series coupled with an IRMS; Finnigan Delta Plus XP; Thermo Scientific).

Single-cell analysis. In addition to the sample for IRMS measurements, extra samples from the last time point of the stable isotope incubation experiments were filtered onto gold-palladium-precoated polycarbonate filters (0.2-μm pore size; Millipore, Germany) for FISH-secondary ion mass spectrometry (SIMS) analysis. Select field of views containing hybridized cells were marked using laser dissection microscopy (DM 6000 B, Leica, Germany) and analyzed by nanoSIMS (nanoSIMS 50L; Cameca, France), which was used to measure simultaneously the single-cell isotopic composition of Arc94-hybridized cells. Secondary ions ^{12}C, ^{13}C, ^{19}F, $^{12}C^{14}N$, $^{12}C^{15}N$, ^{31}P, and ^{32}S were measured on 7 mass detectors. Samples were presputtered with a Cs^+ primary ion beam of ~300 pA, and thereafter, the instrument was tuned on a 50- by 50-μm-field-of-view raster size (yielding a mass resolution of over 8,000). Final image acquisition was performed with a primary beam between 1 and 2 pA at a 10- by 10-μm raster size (256 × 256 pixels) with a dwell time of 1 ms per pixel for 40 planes.

The $^{13}C/^{12}C$ and $^{32}S/(^{12}C + ^{13}C)$ ratios were calculated using look@nanoSIMS software as outlined elsewhere (71). The ^{19}F signal (of the halogenated oligonucleotide Arc94 probe) was used to specifically identify *Arcobacter* hybridized cells (Fig. 6a). Single-cell carbon assimilation rates were determined using $^{13}C/^{12}C$ enrichment, the labeling percentage, the cell volume (based on a rounded rod consisting of two half spheres), and the cell carbon content (calculated using an allometric model, in which the number of femtograms of C $cell^{-1}$ is equal to $133.754 \times V^{0.438}$, where V is the cell biovolume [in cubic micrometers] [72]) and divided over the incubation period.

Enrichment of *Arcobacter*. The *Arcobacter* culture used in this study was enriched from sulfidic station U1a (Fig. 1; Table S1) at a 50-m depth onboard the research vessel. We used sterile-filtered Peru seawater with additions of sodium nitrate and either sodium sulfite, sodium thiosulfate, or elemental sulfur as electron donors to a final concentration of 100 μM. A total of three transfers were made (with a 1% [vol/vol] inoculum) into new medium over the course of the research campaign, and samples were incubated in the dark at 14°C onboard the research vessel. Samples at ~4°C along with additional filter-sterilized Peruvian seawater were express delivered (arriving within 2 to 3 days) to the laboratory at the Max Planck Institute for Marine Microbiology in Bremen, Germany. The enrichment cultures were maintained using 0.2-μm-pore-size filtered and autoclaved anaerobic (N_2-CO_2 atmosphere) Peruvian seawater. After autoclaving, the medium was supplemented with sulfide and nitrate (~80 μM), inoculated (with a 1% [vol/vol] inoculum), and then incubated at close to ambient water temperatures (14°C). Sulfide and nitrate concentrations were monitored, and once the medium was consumed, the cultures were transferred to fresh medium. After five transfers (1% [vol/vol] inoculum) on nitrate and dissolved sulfide, based on the CARD-FISH screening using the Arc94 probe, *Arcobacter* cells made up 90 to 95% of the microbial community. Genomic DNA was then extracted from the nearly pure *Arcobacter* culture using a QIAamp genomic DNA kit (Qiagen, Netherlands).

Genome sequencing and analysis. Whole-genome sequencing on culture-extracted genomic DNA was performed using the Pacific Biosciences RS II technology (P4-C2 chemistry; Max Planck Genome Center, Cologne, Germany). The collected data were processed and filtered using SMRT analysis software (v.2.1). For genome assembly, SMRT analysis routine HGAP2 was applied. From the polished assembly of the sequences obtained by the use of PacBio, contigs shorter than 10 kbp were excluded, resulting in a single, long contig. For genome circularization and polishing, identical sequences on both contig ends were identified by blastn analysis and trimmed from the genome. Annotation was performed using the RAST program (73), and the annotation of the key metabolic genes was manually inspected and refined. Further analysis of the annotated genome was performed using both the RAST and Pathway tools (74). Genome completeness and contamination were estimated using the CheckM (v.1.0.11 11) tool (44) running the lineage-specific workflow using 338 marker genes.

Isolation. The enriched *Arcobacter* strain (PSE-93) was further maintained on sterile anaerobic North Sea seawater (saNS medium) prepared in a Widdel flask, in which the medium was filter sterilized, autoclaved, and then allowed to cool under an N_2-CO_2 (90:10) atmosphere. The saNS medium was buffered to a final concentration of 2 mM HCO_3^-. Sulfide and nitrate (~80 μM) were amended to the medium, which was eventually dispensed into smaller serum bottles under an N_2-CO_2 atmosphere and inoculated with a 1% (vol/vol) culture from Peruvian seawater medium. The isolation of *Arcobacter* strain PSE-93 was performed by plating on DSMZ 1071 PY-BROTH medium (DSMZ, Germany) supplemented with 200 μM KH_2PO_4, 10 mM $MgSO_4 \cdot 7H_2O$, 5 mM HEPES at a final pH of 7.8 and solidified with Bacto agar (1%, wt/vol). The plates were incubated at 14°C under oxic conditions. After a few weeks of incubation, single colonies were picked and restreaked on new plates until an axenic culture of PSE-93 was obtained, as confirmed by full 16S rRNA in-house Sanger sequencing and microscopic evaluation. Colonies from the axenic PSE-93 culture were thereafter used for inoculation of fresh sterile saNS medium with 50 to 100 μM nitrate and sulfide. PSE-93 was also grown on synthetic seawater (Sas) medium. Sas medium was prepared in a Widdel flask and contained, per liter of deionized water, 27.5 g NaCl, 5 g $MgCl_2 \cdot 6H_2O$, 4.1 g $MgSO_4 \cdot 7H_2O$, 0.66 g $CaCl_2 \cdot 2H_2O$, and 1.02 g KCl (75). The medium was autoclaved and allowed to cool under an N_2-CO_2 (90:10) atmosphere. After cooling, sterile trace element, vitamin, and mineral solutions were added as described by Kamp et al. (75). The medium was buffered by the addition HCO_3^- (to a final concentration of 2 mM), and the pH was adjusted to 7.5.

Physiology experiments. For the time course experiments, the medium was dispensed anaerobically under N_2-CO_2 using Hungate techniques into sterile Duran bottles that were mounted and sealed at the top with a 50-ml glass syringe (SGE Analytical Science, Australia). Duran bottles, including the connected syringe, were filled without a headspace. In addition to the PSE-93 inoculum (1%, vol/vol), organic matter compounds glucose (1%, wt/vol), yeast extract (1%, wt/vol), and [^{13}C]acetate (100 μM), as well as inorganic substrates sulfide (100 μM), nitrate (100 μM; 50% ^{15}N labeling), and bicarbonate (2 mM; 10% ^{13}C labeling), were added via a sidearm port in different combinations (Table 1). Experiments were run at 14°C, mimicking *in situ* conditions. Regular subsamples were taken via the sidearm port over the course of the experiment for the analysis of sulfide, nitrate, and nitrite production (1 ml subsample fixed in 500 μl 5% $ZnCl_2$) as well as for the analysis of labeled N_2 production (1 ml subsample in 12-ml Exetainer glass vials with a helium atmosphere and 50 μl saturated $HgCl_2$ solution). Additionally, 1 ml subsample was fixed in 100 μl 20% paraformaldehyde (PFA) for cell count analysis. At the end of the experiment, the remaining contents of the incubation were filtered onto a precombusted Whatman glass microfiber grade GF/F filter (GE Healthcare Life Sciences, UK) and stored at −20°C until further analysis. Samples for N_2 measurements were stored cap down in the dark at room temperature.

Dissolved sulfide concentrations in $ZnCl_2$-fixed samples were determined photometrically as described above. Nitrate and nitrite concentrations were determined with a CLD 60 chemiluminescence NO/NO_x analyzer (Eco Physics AG, Switzerland) after reduction to NO with acidic sodium iodide (NaI) and acidic vanadium(II) chloride, respectively (76, 77). Isotopic ratios of $^{15}N^{15}N$, $^{15}N^{14}N$, and $^{14}N^{14}N$ nitrogen gas were measured on a gas chromatography (GC) isotope-ratio mass spectrometer (IRMS) (VG Optima, Manchester, UK). Cell counts were obtained by flow cytometry on a BD FACSCalibur system (BD Biosciences, CA, USA) after the 2% PFA-fixed cells were stained for 20 min with SYBR green DNA stain. The instrument flow rate was calibrated with saNS medium. The sampling time was 1 min, and the background was determined with samples from the uninoculated control bottles. To quantify the amounts of ^{15}N and ^{13}C incorporated into biomass, the GFF filters were decalcified overnight, dried at 60°C for 1 h, pelletized into tin cups, and analyzed by use of a Thermo Flash EA 1112 elemental analyzer coupled to an isotopic-ratio mass spectrometer (Finnigan Delta Plus XP; Thermo Fisher Scientific, USA).

Data availability. This Whole Genome Shotgun project and the 16S rRNA gene sequences (clone library) have been deposited in the DDBJ/ENA/GenBank databases under accession numbers CP032363 and MH916845 to MH916849, respectively. Water column nutrients and physical data for the RV *Meteor* M93 Research Expedition are available at Pangaea (https://doi.pangaea.de/10.1594/PANGAEA.860727), while station sulfur chemistry, *Arcobacter* cell densities, and rate process measurements have been submitted to Pangea (https://doi.pangaea.de/10.1594/PANGAEA.894324). Additional data regarding SUP05 cell densities can be found at https://doi.pangaea.de/10.1594/PANGAEA.876062.

SUPPLEMENTAL MATERIAL

Supplemental material for this article may be found at https://doi.org/10.1128/AEM.01344-19.

SUPPLEMENTAL FILE 1, PDF file, 0.3 MB.

ACKNOWLEDGMENTS

We are grateful to the Peruvian authorities for access to their national waters and to the captain and crew of RV *Meteor* Research Expedition M93.

C.M.C., G.L., R.A.S., and M.M.M.K. designed the study; C.M.C., C.P., B.V., H.S., S.L., P.F.H., and T.K. performed the experiments; C.M.C., C.P., G.L., B.V., T.G.F., B.M.F., P.F.H., S.L., T.K., and J.S.G. analyzed the data; C.M.C. and T.G.F. wrote the manuscript with substantial input from G.L., B.M.F., J.S.G., B.V., R.A.S., and M.M.M.K.

We thank G. Klockgether, D. Tienken, A. Schwedt, S. Haas, and K. Latham for analytical and laboratory assistance and C. Schelten for administrative support. A. Oren graciously assisted with the derivation of the species name *A. peruensis*. We thank the Max Planck Genome Centre Cologne (http://mpgc.mpipz.mpg.de/home/) for performing the genomic analysis in this study.

This work was supported by the Max Planck Society; the German National Science Foundation (DFG) Sonderforschungsbereich (SFB754) GEOMAR, Kiel, Germany; and a Natural Sciences and Engineering Research Council of Canada (NSERC) scholarship to C.M.C. B.V. was supported by a European Research Council Starting Grant (640422).

REFERENCES

1. Wirsen CO, Sievert SM, Cavanaugh CM, Molyneaux SJ, Ahmad A, Taylor LT, DeLong EF, Taylor CD. 2002. Characterization of an autotrophic sulfide-oxidizing marine Arcobacter sp. that produces filamentous sulfur. Appl Environ Microbiol 68:316–325. https://doi.org/10.1128/aem.68.1.316-325.2002.
2. Madrid VM, Taylor GT, Scranton MI, Chistoserdov AY. 2001. Phylogenetic diversity of bacterial, and archaeal communities in the anoxic zone of the Cariaco Basin. Appl Environ Microbiol 67:1663–1674. https://doi.org/10.1128/AEM.67.4.1663-1674.2001.
3. Borin S, Brusetti L, Mapelli F, D'Auria G, Brusa T, Marzorati M, Rizzi A, Yakimov M, Marty D, De Lange GJ, Van der Wielen P, Bolhuis H, McGenity TJ, Polymenakou PN, Malinverno E, Giuliano L, Corselli C, Daffonchio D. 2009. Sulfur cycling and methanogenesis primarily drive microbial colonization of the highly sulfidic Urania deep hypersaline basin. Proc Natl Acad Sci U S A 106:9151–9156. https://doi.org/10.1073/pnas.0811984106.
4. Fuchsman CA, Murray JW, Staley JT. 2012. Stimulation of autotrophic denitrification by intrusions of the Bosporus plume into the anoxic Black Sea. Front Microbiol 3:257. https://doi.org/10.3389/fmicb.2012.00257.
5. Berg C, Beckmann S, Jost G, Labrenz M, Jürgens K. 2013. Acetate-utilizing bacteria at an oxic–anoxic interface in the Baltic Sea. FEMS Microbiol Ecol 85:251–261. https://doi.org/10.1111/1574-6941.12114.
6. Lavik G, Stuhrmann T, Bruchert V, Van der Plas A, Mohrholz V, Lam P, Mussmann M, Fuchs BM, Amann R, Lass U, Kuypers MM. 2009. Detoxification of sulphidic African shelf waters by blooming chemolithotrophs. Nature 457:581–584. https://doi.org/10.1038/nature07588.
7. Llobet-Brossa E, Rosselló-Mora R, Amann R. 1998. Microbial community composition of Wadden Sea sediments as revealed by fluorescence in situ hybridization. Appl Environ Microbiol 64:2691–2696.
8. Vandieken V, Thamdrup B. 2013. Identification of acetate-oxidizing bacteria in a coastal marine surface sediment by RNA-stable isotope probing in anoxic slurries and intact cores. FEMS Microbiol Ecol 84:373–386. https://doi.org/10.1111/1574-6941.12069.
9. Gevertz D, Telang AJ, Voordouw G, Jenneman GE. 2000. Isolation and characterization of strains CVO and FWKO B, two novel nitrate-reducing, sulfide-oxidizing bacteria isolated from oil field brine. Appl Environ Microbiol 66:2491–2501. https://doi.org/10.1128/aem.66.6.2491-2501.2000.
10. Roalkvam I, Drønen K, Stokke R, Daae FL, Dahle H, Steen IH. 2015. Physiological and genomic characterization of Arcobacter anaerophilus IR-1 reveals new metabolic features in Epsilonproteobacteria. Front Microbiol 6:987. https://doi.org/10.3389/fmicb.2015.00987.
11. Miller WG, Parker CT, Rubenfield M, Mendz GL, Wösten M, Ussery DW, Stolz JF, Binnewies TT, Hallin PF, Wang G, Malek JA, Rogosin A, Stanker LH, Mandrell RE. 2007. The complete genome sequence and analysis of the epsilonproteobacterium Arcobacter butzleri. PLoS One 2:e1358. https://doi.org/10.1371/journal.pone.0001358.
12. Lee C, Agidi S, Marion JW, Lee J. 2012. Arcobacter in Lake Erie beach waters: an emerging gastrointestinal pathogen linked with human-associated fecal contamination. Appl Environ Microbiol 78:5511–5519. https://doi.org/10.1128/AEM.08009-11.
13. Ferreira S, Queiroz JA, Oleastro M, Domingues FC. 2016. Insights in the pathogenesis and resistance of Arcobacter: a review. Crit Rev Microbiol 42:364–383. https://doi.org/10.3109/1040841X.2014.954523.
14. Collado L, Figueras MJ. 2011. Taxonomy, epidemiology, and clinical relevance of the genus Arcobacter. Clin Microbiol Rev 24:174–192. https://doi.org/10.1128/CMR.00034-10.
15. Callbeck C, Dong X, Chatterjee I, Agrawal A, Caffrey S, Sensen C, Voordouw G. 2011. Microbial community succession in a bioreactor modeling a souring low-temperature oil reservoir subjected to nitrate injection. Appl Microbiol Biotechnol 91:799–810. https://doi.org/10.1007/s00253-011-3287-2.
16. Gieg L, Jack T, Foght J. 2011. Biological souring and mitigation in oil reservoirs. Appl Microbiol Biotechnol 92:263–282. https://doi.org/10.1007/s00253-011-3542-6.
17. Hubert CRJ, Oldenburg TBP, Fustic M, Gray ND, Larter SR, Penn K, Rowan AK, Seshadri R, Sherry A, Swainsbury R, Voordouw G, Voordouw JK, Head IM. 2012. Massive dominance of Epsilonproteobacteria in formation waters from a Canadian oil sands reservoir containing severely biodegraded oil. Environ Microbiol 14:387–404. https://doi.org/10.1111/j.1462-2920.2011.02521.x.
18. Hamann E, Gruber-Vodicka H, Kleiner M, Tegetmeyer HE, Riedel D, Littmann S, Chen J, Milucka J, Viehweger B, Becker KW, Dong X, Stairs CW, Hinrichs K-U, Brown MW, Roger AJ, Strous M. 2016. Environmental Breviatea harbour mutualistic Arcobacter epibionts. Nature 534:254–258. https://doi.org/10.1038/nature18297.
19. Sievert SM, Wieringa EBA, Wirsen CO, Taylor CD. 2007. Growth and mechanism of filamentous-sulfur formation by Candidatus Arcobacter sulfidicus in opposing oxygen-sulfide gradients. Environ Microbiol 9:271–276. https://doi.org/10.1111/j.1462-2920.2006.01156.x.
20. Grünke S, Felden J, Lichtschlag A, Girnth AC, De Beer D, Wenzhöfer F, Boetius A. 2011. Niche differentiation among mat-forming, sulfide-oxidizing bacteria at cold seeps of the Nile Deep Sea Fan (eastern Mediterranean Sea). Geobiology 9:330–348. https://doi.org/10.1111/j.1472-4669.2011.00281.x.
21. Kalenitchenko D, Dupraz M, Le Bris N, Petetin C, Rose C, West NJ, Galand PE. 2016. Ecological succession leads to chemosynthesis in mats colonizing wood in sea water. ISME J 10:2246–2258. https://doi.org/10.1038/ismej.2016.12.
22. Fossing H. 1990. Sulfate reduction in shelf sediments in the upwelling region off Central Peru. Continental Shelf Res 10:355–367. https://doi.org/10.1016/0278-4343(90)90056-R.
23. Böning P, Brumsack H-J, Böttcher ME, Schnetger B, Kriete C, Kallmeyer J, Borchers SL. 2004. Geochemistry of Peruvian near-surface sediments. Geochim Cosmochim Acta 68:4429–4451. https://doi.org/10.1016/j.gca.2004.04.027.
24. Sommer S, Gier J, Treude T, Lomnitz U, Dengler M, Cardich J, Dale AW. 2016. Depletion of oxygen, nitrate and nitrite in the Peruvian oxygen

minimum zone cause an imbalance of benthic nitrogen fluxes. Deep Sea Res Part I Oceanogr Res Pap 112:113–122. https://doi.org/10.1016/j.dsr.2016.03.001.
25. Brüchert V, Currie B, Peard KR. 2009. Hydrogen sulphide and methane emissions on the central Namibian shelf. Prog Oceanogr 83:169–179. https://doi.org/10.1016/j.pocean.2009.07.017.
26. Schunck H, Lavik G, Desai DK, Großkopf T, Kalvelage T, Löscher CR, Paulmier A, Contreras S, Siegel H, Holtappels M, Rosenstiel P, Schilhabel MB, Graco M, Schmitz RA, Kuypers MMM, Laroche J. 2013. Giant hydrogen sulfide plume in the oxygen minimum zone off Peru supports chemolithoautotrophy. PLoS One 8:e68661. https://doi.org/10.1371/journal.pone.0068661.
27. Callbeck CM, Lavik G, Ferdelman TG, Fuchs B, Gruber-Vodicka HR, Hach PF, Littmann S, Schoffelen NJ, Kalvelage T, Thomsen S, Schunck H, Löscher CR, Schmitz RA, Kuypers MM. 2018. Oxygen minimum zone cryptic sulfur cycling sustained by offshore transport of key sulfur oxidizing bacteria. Nat Commun 9:1729. https://doi.org/10.1038/s41467-018-04041-x.
28. Galán A, Faúndez J, Thamdrup B, Santibáñez JF, Farías L. 2014. Temporal dynamics of nitrogen loss in the coastal upwelling ecosystem off central Chile: evidence of autotrophic denitrification through sulfide oxidation. Limnol Oceanogr 59:1865–1878. https://doi.org/10.4319/lo.2014.59.6.1865.
29. Naqvi SW, Jayakumar DA, Narvekar PV, Naik H, Sarma VV, D'Souza W, Joseph S, George MD. 2000. Increased marine production of N_2O due to intensifying anoxia on the Indian continental shelf. Nature 408:346–349. https://doi.org/10.1038/35042551.
30. Rabalais NN, Turner RE, Scavia D. 2002. Beyond science into policy: Gulf of Mexico hypoxia and the Mississippi River: nutrient policy development for the Mississippi River watershed reflects the accumulated scientific evidence that the increase in nitrogen loading is the primary factor in the worsening of hypoxia in the northern Gulf of Mexico. Bioscience 52:129–142. https://doi.org/10.1641/0006-3568(2002)052[0129:BSIPGO]2.0.CO;2.
31. Diaz RJ, Rosenberg R. 2008. Spreading dead zones and consequences for marine ecosystems. Science 321:926–929. https://doi.org/10.1126/science.1156401.
32. Breitburg D, Levin LA, Oschlies A, Grégoire M, Chavez FP, Conley DJ, Garçon V, Gilbert D, Gutiérrez D, Isensee K, Jacinto GS, Limburg KE, Montes I, Naqvi SWA, Pitcher GC, Rabalais NN, Roman MR, Rose KA, Seibel BA, Telszewski M, Yasuhara M, Zhang J. 2018. Declining oxygen in the global ocean and coastal waters. Science 359:eaam7240. https://doi.org/10.1126/science.aam7240.
33. Copenhagen WJ. 1954. The periodic mortality of fish in the Walvis region. S Afr Med J 28:381.
34. Levin LA, Ekau W, Gooday AJ, Jorissen F, Middelburg JJ, Naqvi SWA, Neira C, Rabalais NN, Zhang J. 2009. Effects of natural and human-induced hypoxia on coastal benthos. Biogeosciences 6:2063–2098. https://doi.org/10.5194/bg-6-2063-2009.
35. Taylor GT, Iabichella M, Ho T-Y, Scranton MI, Thunell RC, Muller-Karger F, Varela R. 2001. Chemoautotrophy in the redox transition zone of the Cariaco Basin: a significant midwater source of organic carbon production. Limnol Oceanogr 46:148–163. https://doi.org/10.4319/lo.2001.46.1.0148.
36. Glaubitz S, Labrenz M, Jost G, Jurgens K. 2010. Diversity of active chemolithoautotrophic prokaryotes in the sulfidic zone of a Black Sea pelagic redoxcline as determined by rRNA-based stable isotope probing. FEMS Microbiol Ecol 74:32–41. https://doi.org/10.1111/j.1574-6941.2010.00944.x.
37. Zopfi J, Ferdelman TG, Jorgensen BB, Teske A, Thamdrup B. 2001. Influence of water column dynamics on sulfide oxidation and other major biogeochemical processes in the chemocline of Mariager Fjord (Denmark). Mar Chem 74:29–51. https://doi.org/10.1016/S0304-4203(00)00091-8.
38. Glaubitz S, Lueders T, Abraham WR, Jost G, Jurgens K, Labrenz M. 2009. ^{13}C-isotope analyses reveal that chemolithoautotrophic Gamma- and Epsilonproteobacteria feed a microbial food web in a pelagic redoxcline of the central Baltic Sea. Environ Microbiol 11:326–337. https://doi.org/10.1111/j.1462-2920.2008.01770.x.
39. Löscher CR, Bange HW, Schmitz RA, Callbeck CM, Engel A, Hauss H, Kanzow T, Kiko R, Lavik G, Loginova A, Melzner F, Meyer J, Neulinger SC, Pahlow M, Riebesell U, Schunck H, Thomsen S, Wagner H. 2016. Water column biogeochemistry of oxygen minimum zones in the eastern tropical North Atlantic and eastern tropical South Pacific Oceans. Biogeosciences 13:3585–3606. https://doi.org/10.5194/bg-13-3585-2016.
40. Brüchert V, Currie B, Peard KR, Lass U, Endler R, Dübecke A, Julies E, Leipe T, Zitzmann S. 2006. Biogeochemical and physical control on shelf anoxia and water column hydrogen sulphide in the Benguela upwelling system of Namibia, p 161–193. *In* Neretin NL (ed), Past and present water column anoxia. Springer, Dordrecht, Netherlands. https://doi.org/10.1007/1-4020-4297-3_07.
41. Callbeck C. 2017. Distribution and activity of anammox and sulfide-oxidizing nitrate-reducing bacteria in oxygen minimum zones. PhD dissertation. Max Planck Institute for Marine Microbiology/University of Bremen, Bremen, Germany.
42. Taylor CD, Wirsen CO. 1997. Microbiology and ecology of filamentous sulfur formation. Science 277:1483–1485. https://doi.org/10.1126/science.277.5331.1483.
43. Moussard H, Corre E, Cambon-Bonavita M-A, Fouquet Y, Jeanthon C. 2006. Novel uncultured Epsilonproteobacteria dominate a filamentous sulphur mat from the 13°N hydrothermal vent field, East Pacific Rise. FEMS Microbiol Ecol 58:449–463. https://doi.org/10.1111/j.1574-6941.2006.00192.x.
44. Parks DH, Imelfort M, Skennerton CT, Hugenholtz P, Tyson GW. 2015. CheckM: assessing the quality of microbial genomes recovered from isolates, single cells, and metagenomes. Genome Res 25:1043–1055. https://doi.org/10.1101/gr.186072.114.
45. Aussignargues C, Giuliani MC, Infossi P, Lojou E, Guiral M, Giudici-Orticoni MT, Ilbert M. 2012. A rhodanese functions as a sulfur supplier for key enzymes in sulfur energy metabolism. J Biol Chem 287:19936. https://doi.org/10.1074/jbc.M111.324863.
46. Dahl C, Engels S, Pott-Sperling AS, Schulte A, Sander J, Lübbe Y, Deuster O, Brune DC. 2005. Novel genes of the dsr gene cluster and evidence for close interaction of Dsr proteins during sulfur oxidation in the phototrophic sulfur bacterium Allochromatium vinosum. J Bacteriol 187:1392–1404. https://doi.org/10.1128/JB.187.4.1392-1404.2005.
47. Klappenbach JA, Dunbar JM, Schmidt TM. 2000. rRNA operon copy number reflects ecological strategies of bacteria. Appl Environ Microbiol 66:1328–1333. https://doi.org/10.1128/aem.66.4.1328-1333.2000.
48. Pérez-Cataluña A, Salas-Massó N, Diéguez AL, Balboa S, Lema A, Romalde JL, Figueras MJ. 2018. Revisiting the taxonomy of the genus Arcobacter: getting order from the chaos. Front Microbiol 9:2077. https://doi.org/10.3389/fmicb.2018.02077.
49. Eilers H, Pernthaler J, Glöckner FO, Amann R. 2000. Culturability and in situ abundance of pelagic bacteria from the North Sea. Appl Environ Microbiol 66:3044–3051. https://doi.org/10.1128/aem.66.7.3044-3051.2000.
50. Pati A, Gronow S, Lapidus A, Copeland A, Rio TGD, Nolan M, Lucas S, Tice H, Cheng J-F, Han C, Chertkov O, Bruce D, Tapia R, Goodwin L, Pitluck S, Liolios K, Ivanova N, Mavromatis K, Chen A, Palaniappan K, Land M, Hauser L, Chang Y-J, Jeffries CD, Detter JC, Rohde M, Göker M, Bristow J, Eisen JA, Markowitz V, Hugenholtz P, Klenk H-P, Kyrpides NC. 2010. Complete genome sequence of Arcobacter nitrofigilis type strain (CI T). Stand Genomic Sci 2:300–308. https://doi.org/10.4056/sigs.912121.
51. Ho T-Y, Scranton MI, Taylor GT, Varela R, Thunell RC, Muller-Karger F. 2002. Acetate cycling in the water column of the Cariaco Basin: seasonal and vertical variability and implication for carbon cycling. Limnol Oceanogr 47:1119–1128. https://doi.org/10.4319/lo.2002.47.4.1119.
52. Zhuang GC, Pena-Montenegro TD, Montgomery A, Montoya JP, Joye SB. 2019. Significance of acetate as a microbial carbon and energy source in the water column of Gulf of Mexico: implications for marine carbon cycling. Global Biogeochem Cycles 33:223–235. https://doi.org/10.1029/2018GB006129.
53. Gimenez R, Nuñez MF, Badia J, Aguilar J, Baldoma L. 2003. The gene yjcG, cotranscribed with the gene acs, encodes an acetate permease in Escherichia coli. J Bacteriol 185:6448–6455. https://doi.org/10.1128/jb.185.21.6448-6455.2003.
54. Kumari S, Beatty CM, Browning DF, Busby SJW, Simel EJ, Hovel-Miner G, Wolfe AJ. 2000. Regulation of acetyl coenzyme A synthetase in Escherichia coli. J Bacteriol 182:4173–4179. https://doi.org/10.1128/jb.182.15.4173-4179.2000.
55. Fuchs G, Berg IA. 2014. Unfamiliar metabolic links in the central carbon metabolism. J Biotechnol 192:314–322. https://doi.org/10.1016/j.jbiotec.2014.02.015.
56. Loginova AN, Thomsen S, Engel A. 2016. Chromophoric and fluorescent dissolved organic matter in and above the oxygen minimum zone off Peru. J Geophys Res Oceans 121:7973–7990. https://doi.org/10.1002/2016JC011906.
57. Erb TJ. 2011. Carboxylases in natural and synthetic microbial pathways. Appl Environ Microbiol 77:8466–8477. https://doi.org/10.1128/AEM.05702-11.
58. Kelly DP. 1982. Biochemistry of the chemolithotrophic oxidation of

inorganic sulphur. Philos Trans R Soc Lond B Biol Sci 298:499–528. https://doi.org/10.1098/rstb.1982.0094.
59. Kelly PD. 1999. Thermodynamic aspects of energy conservation by chemolithotrophic sulfur bacteria in relation to the sulfur oxidation pathways. Arch Microbiol 171:219–229. https://doi.org/10.1007/s002030050703.
60. Nelson DC, Jørgensen BB, Revsbech NP. 1986. Growth pattern and yield of a chemoautotrophic Beggiatoa sp. in oxygen-sulfide microgradients. Appl Environ Microbiol 52:225–233.
61. Cline JD. 1969. Spectrophotometric determination of hydrogen sulfide in natural waters. Limnol Oceanogr 14:454–458. https://doi.org/10.4319/lo.1969.14.3.0454.
62. Schlitzer R. 2018. Ocean Data View software. odv.awi.de.
63. Kamyshny A, Zilberbrand M, Ekeltchik I, Voitsekovski T, Gun J, Lev O. 2008. Speciation of polysulfides and zerovalent sulfur in sulfide-rich water wells in southern and central Israel. Aquat Geochem 14:171–192. https://doi.org/10.1007/s10498-008-9031-6.
64. Pruesse E, Peplies J, Glöckner FO. 2012. SINA: accurate high-throughput multiple sequence alignment of ribosomal RNA genes. Bioinformatics 28:1823–1829. https://doi.org/10.1093/bioinformatics/bts252.
65. Quast C, Pruesse E, Yilmaz P, Gerken J, Schweer T, Yarza P, Peplies J, Glöckner FO. 2013. The SILVA ribosomal RNA gene database project: improved data processing and web-based tools. Nucleic Acids Res 41:D590–D596. https://doi.org/10.1093/nar/gks1219.
66. Ludwig W, Strunk O, Westram R, Richter L, Meier H, Yadhukumar, Buchner A, Lai T, Steppi S, Jobb G, Förster W, Brettske I, Gerber S, Ginhart AW, Gross O, Grumann S, Hermann S, Jost R, König A, Liss T, Lüßmann R, May M, Nonhoff B, Reichel B, Strehlow R, Stamatakis A, Stuckmann N, Vilbig A, Lenke M, Ludwig T, Bode A, Schleifer KH. 2004. ARB: a software environment for sequence data. Nucleic Acids Res 32:1363–1371. https://doi.org/10.1093/nar/gkh293.
67. Stamatakis A. 2014. RAxML version 8: a tool for phylogenetic analysis and post-analysis of large phylogenies. Bioinformatics 30:1312–1313. https://doi.org/10.1093/bioinformatics/btu033.
68. Snaidr J, Amann R, Huber I, Ludwig W, Schleifer KH. 1997. Phylogenetic analysis and in situ identification of bacteria in activated sludge. Appl Environ Microbiol 63:2884–2896.
69. Pernthaler A, Pernthaler J, Amann R. 2002. Fluorescence in situ hybridization and catalyzed reporter deposition for the identification of marine bacteria. Appl Environ Microbiol 68:3094–3101. https://doi.org/10.1128/aem.68.6.3094-3101.2002.
70. Callbeck CM, Lavik G, Stramma L, Kuypers MMM, Bristow LA. 2017. Enhanced nitrogen loss by eddy-induced vertical transport in the offshore Peruvian oxygen minimum zone. PLoS One 12:e0170059. https://doi.org/10.1371/journal.pone.0170059.
71. Polerecky L, Adam B, Milucka J, Musat N, Vagner T, Kuypers MM. 2012. Look@NanoSIMS—a tool for the analysis of nanoSIMS data in environmental microbiology. Environ Microbiol 14:1009–1023. https://doi.org/10.1111/j.1462-2920.2011.02681.x.
72. Romanova ND, Sazhin AF. 2010. Relationships between the cell volume and the carbon content of bacteria. Oceanology 50:522–530. https://doi.org/10.1134/S0001437010040089.
73. Aziz RK, Bartels D, Best AA, DeJongh M, Disz T, Edwards RA, Formsma K, Gerdes S, Glass EM, Kubal M, Meyer F, Olsen GJ, Olson R, Osterman AL, Overbeek RA, McNeil LK, Paarmann D, Paczian T, Parrello B, Pusch GD, Reich C, Stevens R, Vassieva O, Vonstein V, Wilke A, Zagnitko O. 2008. The RAST server: rapid annotations using subsystems technology. BMC Genomics 9:75. https://doi.org/10.1186/1471-2164-9-75.
74. Caspi R, Altman T, Dreher K, Fulcher CA, Subhraveti P, Keseler IM, Kothari A, Krummenacker M, Latendresse M, Mueller LA, Ong Q, Paley S, Pujar A, Shearer AG, Travers M, Weerasinghe D, Zhang P, Karp PD. 2012. The MetaCyc database of metabolic pathways and enzymes and the BioCyc collection of pathway/genome databases. Nucleic Acids Res 40:D742–D753. https://doi.org/10.1093/nar/gkr1014.
75. Kamp A, Røy H, Schulz-Vogt HN. 2008. Video-supported analysis of Beggiatoa filament growth, breakage, and movement. Microb Ecol 56:484–491. https://doi.org/10.1007/s00248-008-9367-x.
76. Braman RS, Hendrix SA. 1989. Nanogram nitrite and nitrate determination in environmental and biological materials by vanadium(III) reduction with chemiluminescence detection. Anal Chem 61:2715–2718. https://doi.org/10.1021/ac00199a007.
77. Cox RD. 1980. Determination of nitrate and nitrite at the parts per billion level by chemiluminescence. Anal Chem 52:332–335. https://doi.org/10.1021/ac50052a028.
78. Hügler M, Wirsen CO, Fuchs G, Taylor CD, Sievert SM. 2005. Evidence for autotrophic CO_2 fixation via the reductive tricarboxylic acid cycle by members of the ε subdivision of proteobacteria. J Bacteriol 187:3020–3027. https://doi.org/10.1128/JB.187.9.3020-3027.2005.